Supporting Information

Can surface reactivity of mixed crystals be predicted from their counterparts? A case study of $(Bi_{1-x}Sb_x)_2Te_3$ topological insulators

Andrey A. Volykhov, Jaime Sánchez-Barriga, Maria Batuk, Carolien Callaert, Joke Hadermann, Anna P. Sirotina, Vera S. Neudachina, Alina I. Belova, Nadezhda V. Vladimirova, Marina E. Tamm, Nikolay O. Khmelevsky, Carlos Escudero, Virginia Perez Dieste, Axel Knop-Gericke, Lada V. Yashina

1. Crystal growth and characterisation

The crystal growth was performed in the cylindrical quartz ampoules of 10 mm in diameter with conic tip and heat sink rod. The heat sink rod should be 30–40 mm in length and 4–6 mm in diameter. Closer to the ampoule tip the sink rod becomes narrower, and its diameter becomes 2–3 mm. It is essential that the ampoule walls were uniform, and their thickness did not exceed 2.5 mm. The ampoules were pre-treated with HNO_3+3HCl mixture during 30 min, then washed with distilled water over ten times, dried and heated under the dynamic vacuum conditions. The 6 N-purity elements (Bi, Sb, and Te) were used. Source compositions are given in Table S1. A 10 g mixture of components (purity 5–6 N) was loaded in each of the growth tubes, then the ampoules were sealed off.

The growth furnace had an upper zone with a constant temperature corresponding to melt temperature in Table S1 and a lower zone with a nearly linear decrease of temperature of 10°C/cm. Each ampoule was placed into the lower part of the growth furnace (at a temperature about 50°C below the melting point) and pulled with the velocity of 5 mm/h up to the starting position. This position and the corresponding temperature were preliminary determined by means of visual observation of the solid phase disappearance in the ampoule tip. The ampoule was kept in this position for 0.5–2h, and the melt was periodically mixed; then the ampoule was pulled down with the rates of 1 cm/day. The longitudinal temperature gradient of 10°C/cm from run-to-run was maintained in the growth furnace. After 5–10 days the ampoule was air quenched, with the melt being separated from the crystal.

The composition distribution in the grown crystals was studied both along the axial direction using X-ray fluorescent spectroscopy using reference $(Bi_{1-x}Sb_x)_2Te_3$ samples with different x. The spectra were acquired using Mistral-M1 (Bruker). Crystal composition x seems to be very close to those of the source due to the pronounced tendency to undercooling. Moreover, Sb is uniformly distributed along growth direction. The example is given in Fig.S1.

Table S1. Growth conditions and crystal composition (part of constant concentration)

sample	Source composition			T melt, °C	Initial T crystallization, °C	Duration, days	Crystal composition, x +-0.005
	Bi	Sb	Te				
Sb0	1.98	0	3.04	600	580	5	0
Sb5	1.892	0.108	2.978	605	585	7	0.067

Sb10	1.79	0.21	3.021	610	590	5.5	0.123
Sb25	1.5	0.5	3.075	610	595	8	0.25
Sb40	1.2	0.8	3.007	615	600	6.5	0.388
Sb55	0.892	1.108	3	620	605	7	0.531
Sb55 (Te)	0.9	1.1	3.073	620	605	4	0.535
Sb55(M)	0.902	1.098	2.919	620	605	8	0.529
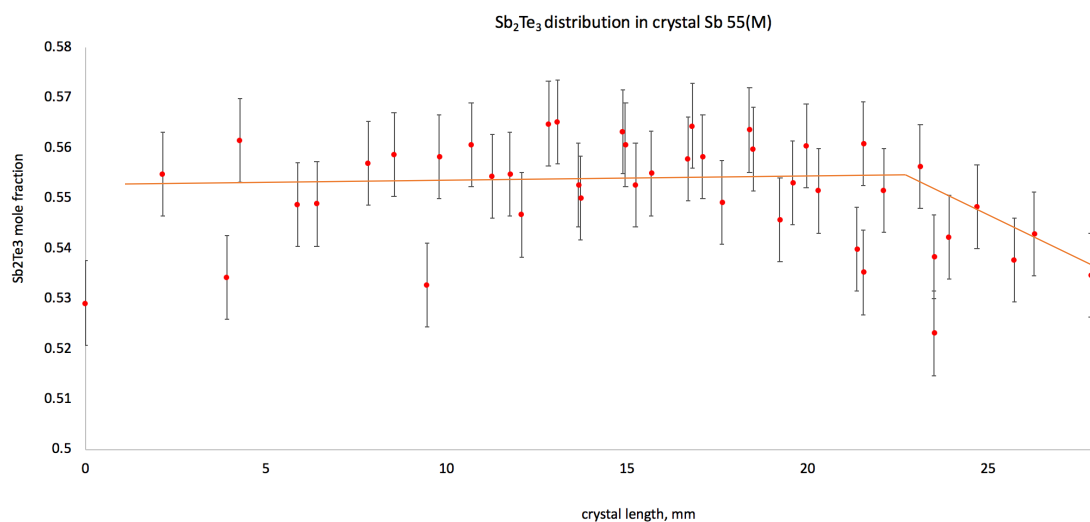
Fig. S1. Typical longitudinal distribution of Sb2Te3 mole fraction in one of the crystal.

2. Atomic scale composition characterisation of bulk crystals
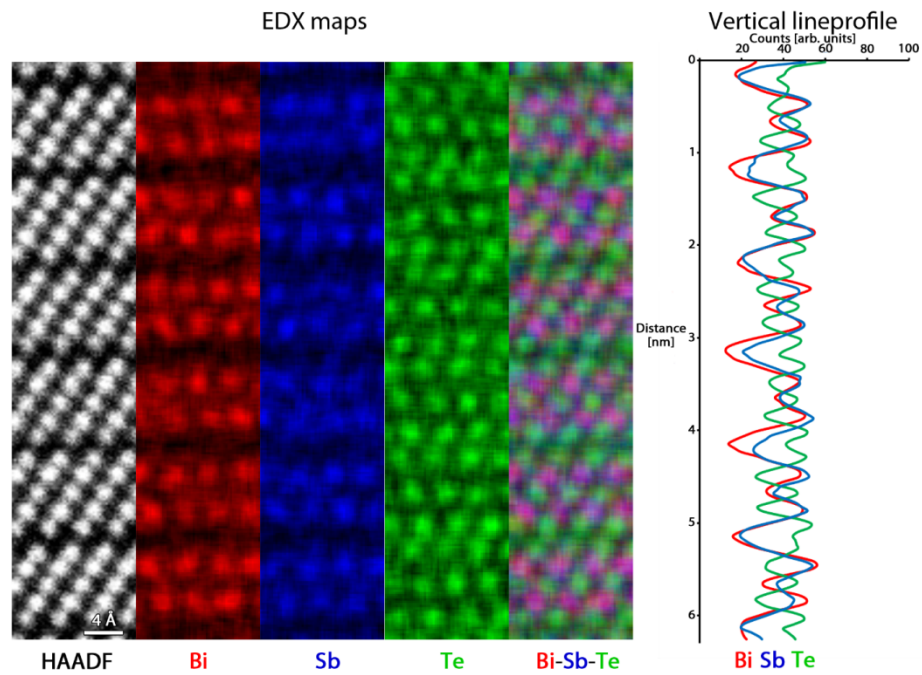
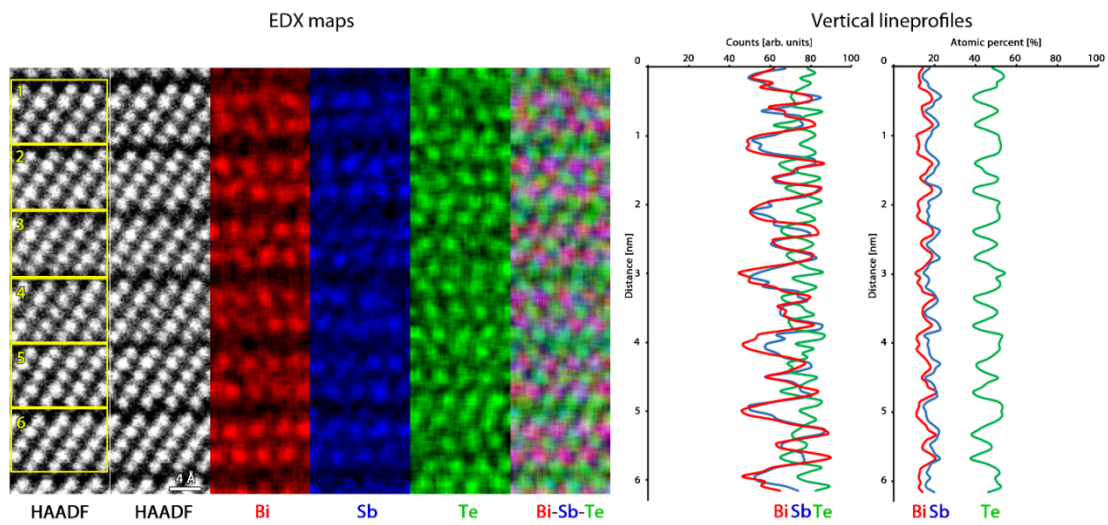Figure S2. Averaged EDX maps (in counts) of two EDX maps of the bulk $(Bi_{0.45}Sb_{0.55})_2Te_3$ crystal with the corresponding line profile.

Figure S3. EDX map in counts (left) of the bulk $(Bi_{0.45}Sb_{0.55})_2Te_3$ crystal of an area in the bulk with the corresponding line profiles in counts and atomic percent (right). The quantification of the areas marked with yellow in the first HAADF-STEM image is given in Table S1.

Table S2. Quantification of different quintuple layers in Fig. S3 and their average.

Area	Bi [at %]	Sb [at %]	Te [at %]	(Bi+Sb)/Te [/]
1	16.7	23.5	59.9	67.1
2	16.4	23.8	59.8	67.1

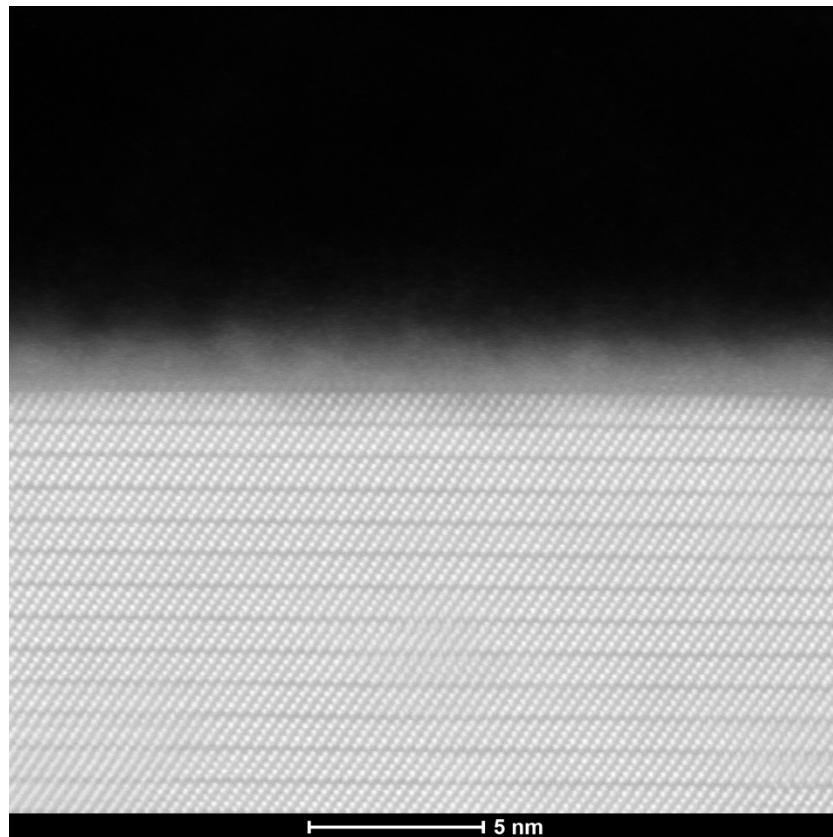|				
3	16.5	22.6	60.9	64.1
4	16.3	23.3	60.5	65.3
5	16.7	23.6	59.7	67.6
6	17.2	23.4	59.4	68.4
Average	16.6	23.3	60.0	66.6

3. Oxide layer and subsurface layer structure

Figure S4. A HAADF-STEM image of the oxide-crystal interface for $(Bi_{0.45}Sb_{0.55})_2Te_3$ after one week of air exposure.
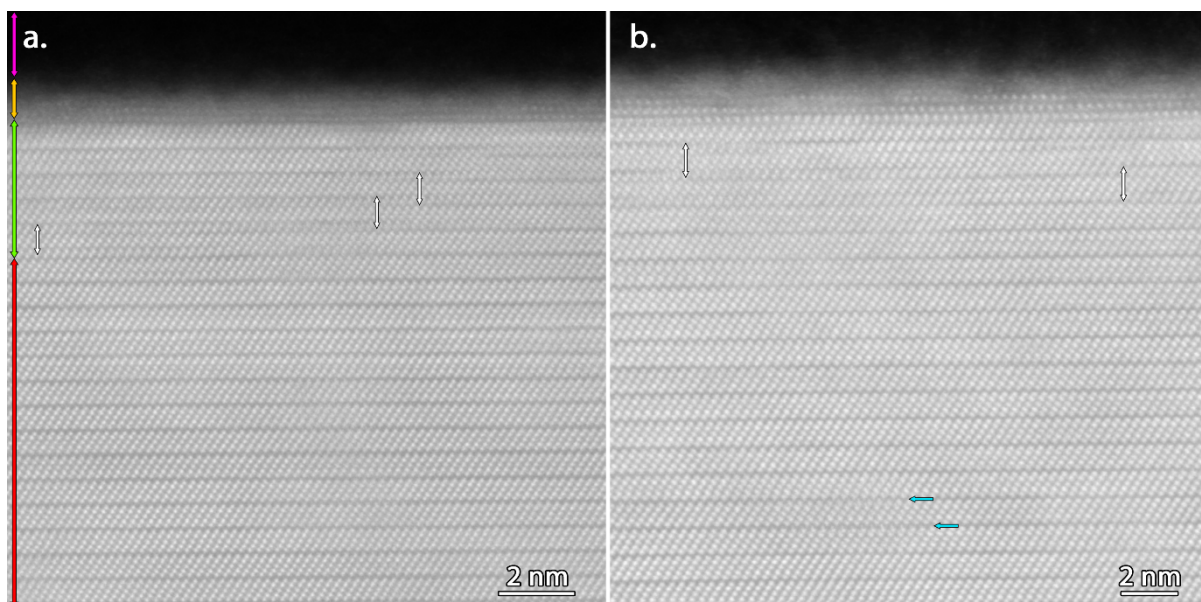
Figure S5. (a) HAADF-STEM image of the oxide-crystal interface for $(Bi_{0.45}Sb_{0.55})_2Te_3$ after about a year of air exposure. White arrows indicate seven-layer lamella. The different layers are marked with different colors: magenta= carbon layer (layer to protect the top of the sample), orange= mostly amorphous top layer with small parts that are still crystalline, green= area with seven-layer lamella and red= area without seven-layer lamella. (b) A HAADF-STEM image where the seven-layer lamellas are marked with white arrows and line defects with cyan arrows.

4. Reactivity descriptor
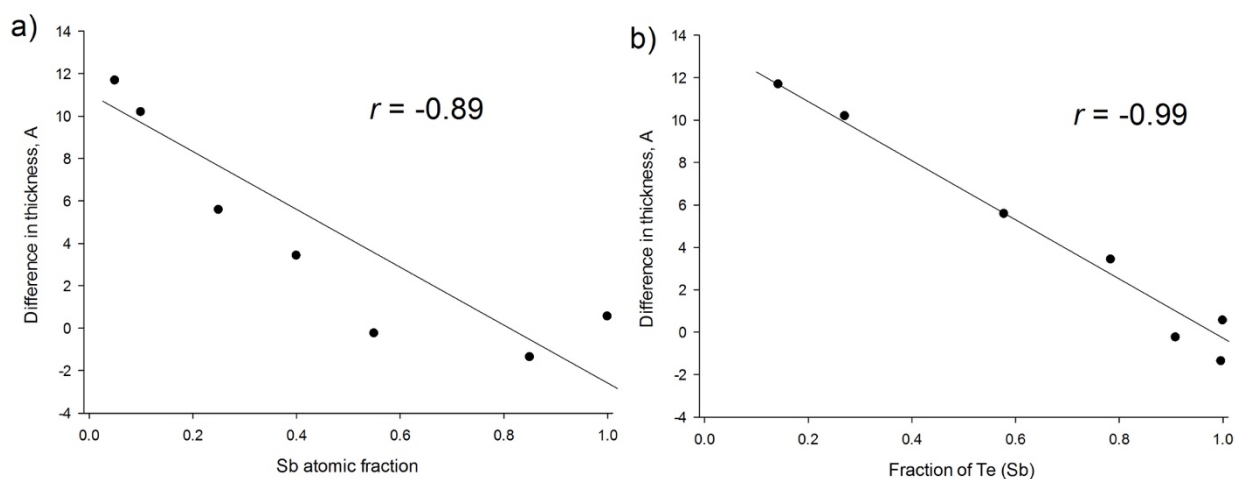
Fig. S6. Reactivity as a function of: a) the crystal composition x, b) fraction of the Te surface atoms bonded with at least one Sb atom.
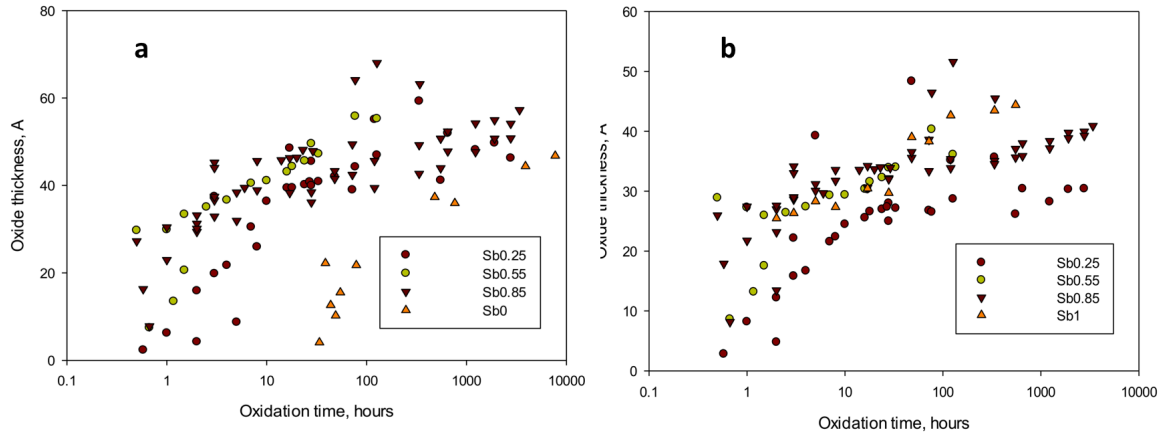
5

5. Oxide layer thickness calculation

Fig. S7. The oxide layer thickness equation from: a) Bi 4f spectra, b) Sb 3d spectra. The layer thickness was calculated as $h = \lambda_0 \ln(\frac{N_s \lambda_s I_0}{N_0 \lambda_0 I_s} + 1)$, where:

λ_o, λ_s – IMFP for the oxide and the substrate layers, respectively, calculated by the TPP2M formula for a specified kinetic energy (averaged for the TeO_2, Sb_2O_3, Bi_2O_3 , Sb_2Te_3 and Bi_2Te_3 in the corresponding ratio)

N_s, N_o are the atomic concentrations of the given atoms in the substrate and the oxide layers, respectively.

I_o, I_s – intensity of the oxidized and non-oxidized components in the XP spectra of a given element, respectively.

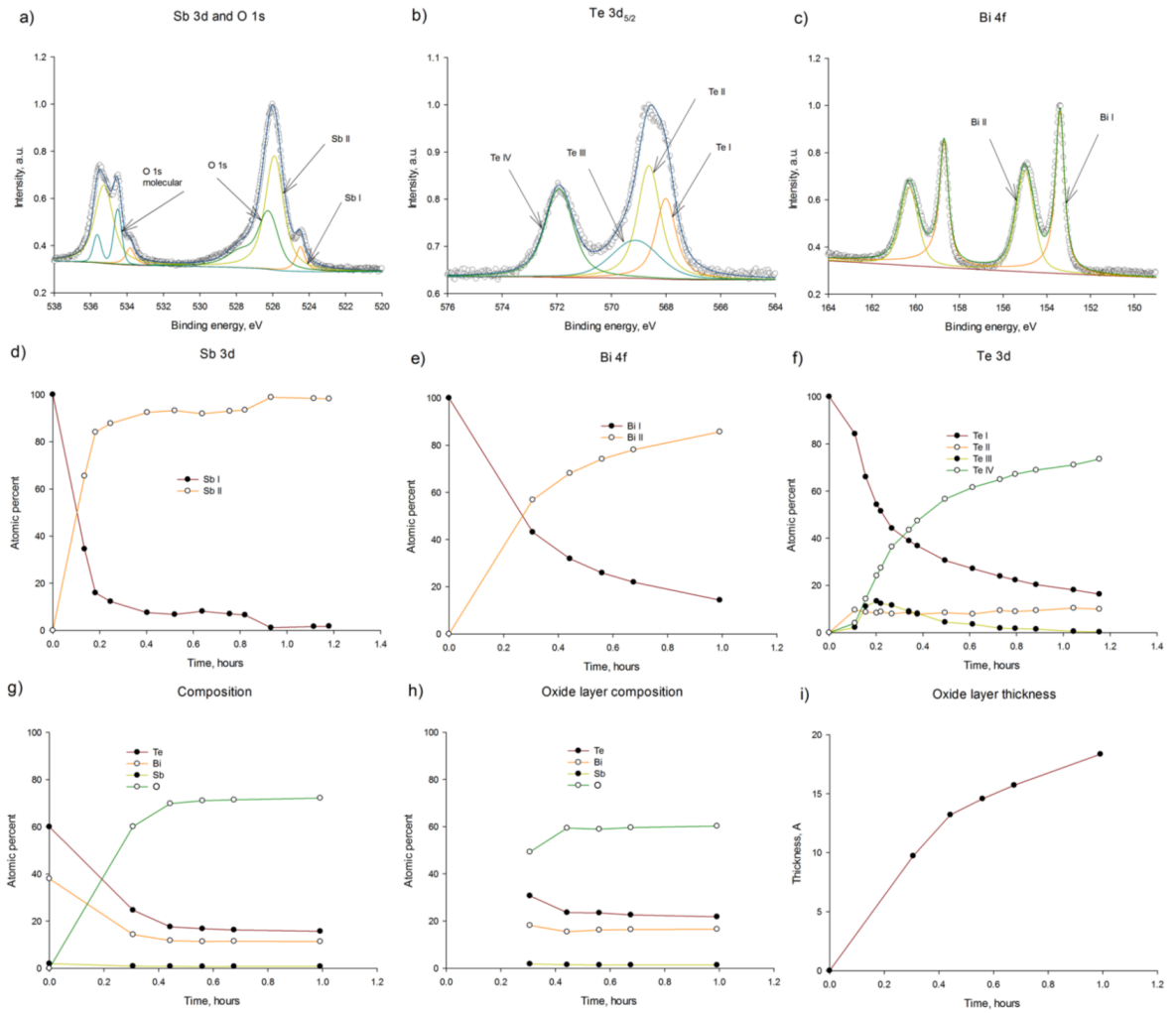## 6. Oxidation kinetics measured *in situ*

Fig. S8. The oxidation kinetics measured in situ for the $(Bi_{0.95}Sb_{0.05})_2Te_3$ crystal surface (KE=200 eV).
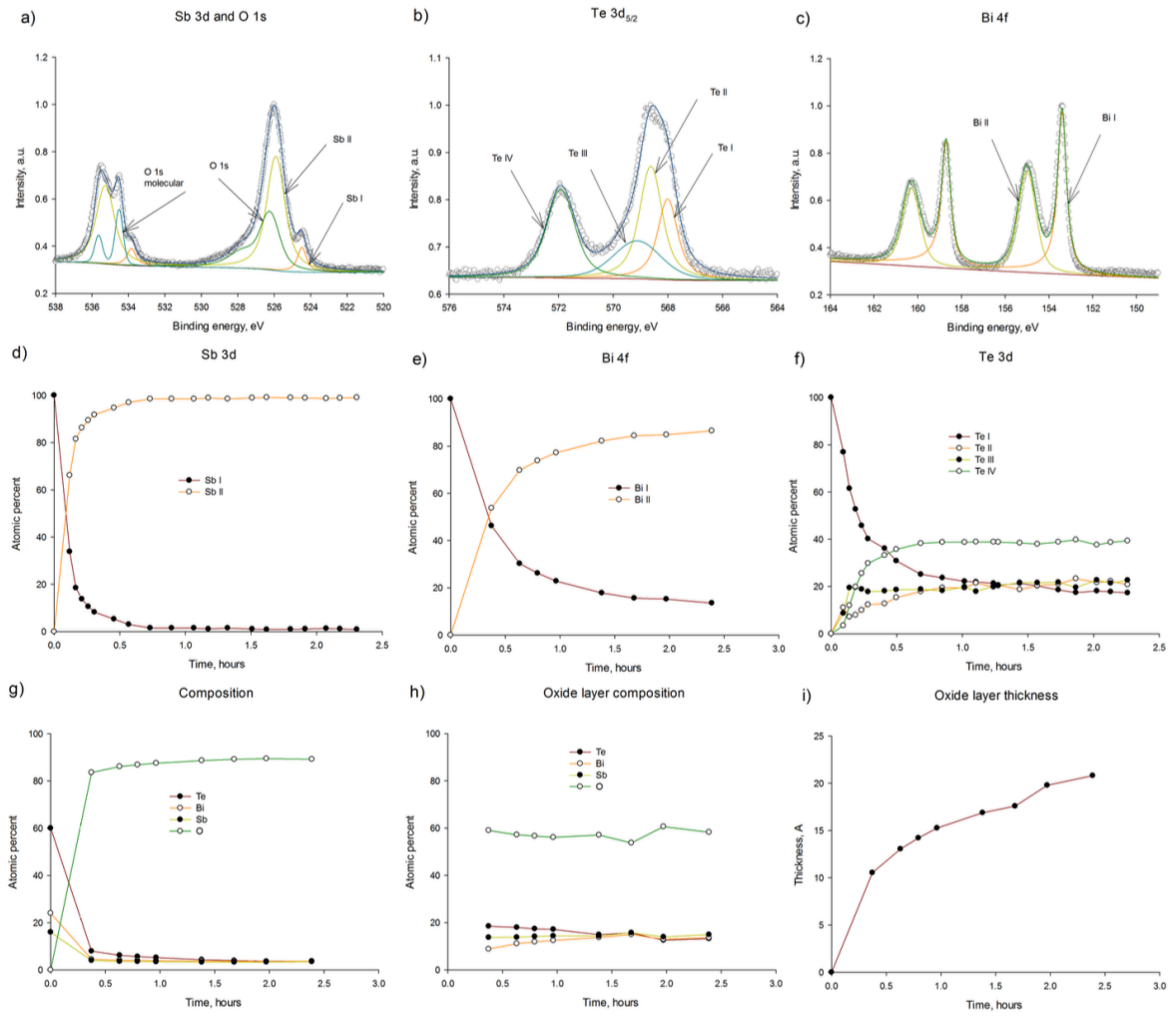
Fig. S9. The oxidation kinetics measured in situ for the $(Bi_{0.6}Sb_{0.4})_2Te_3$ crystal surface (KE=200 eV).

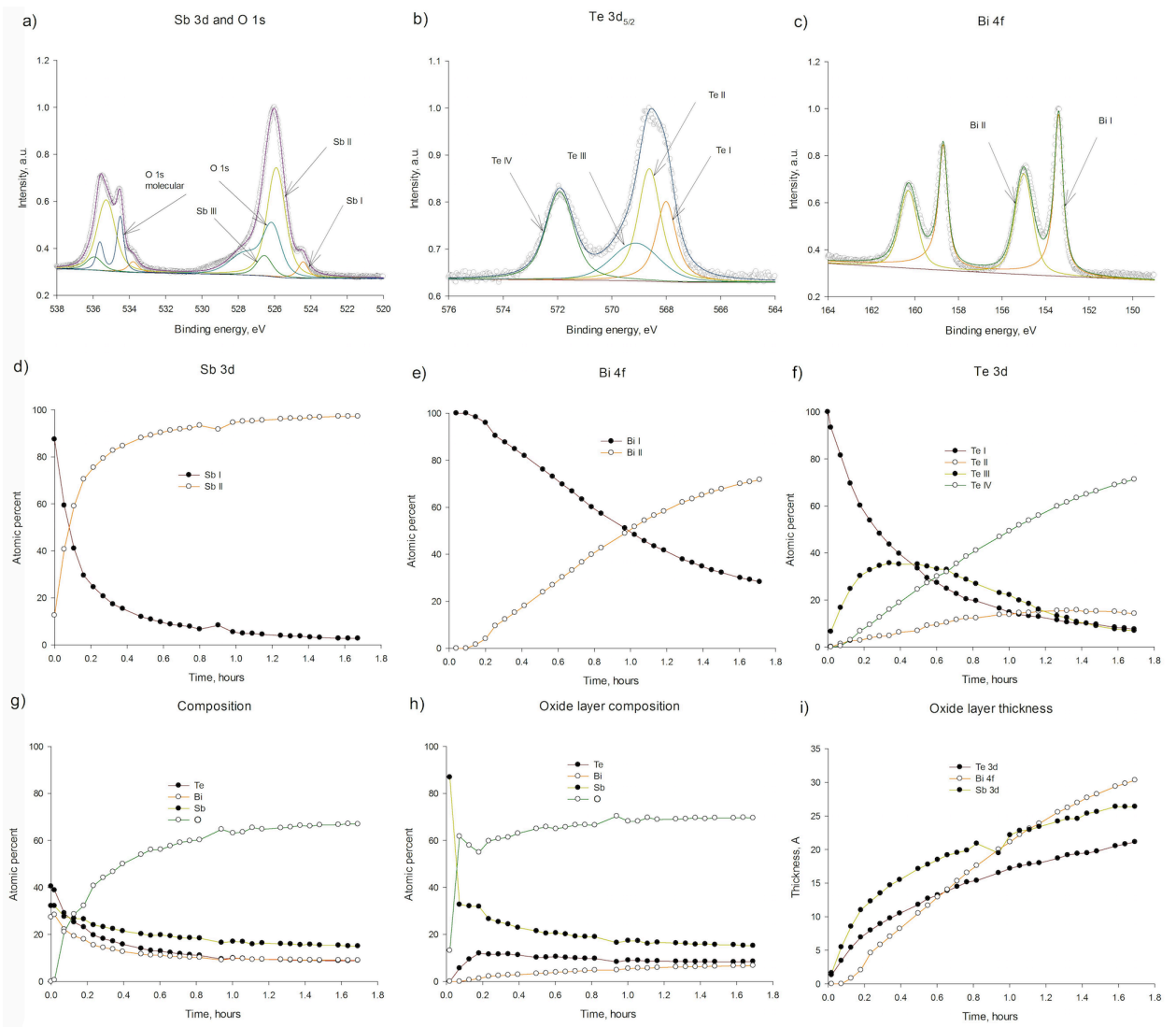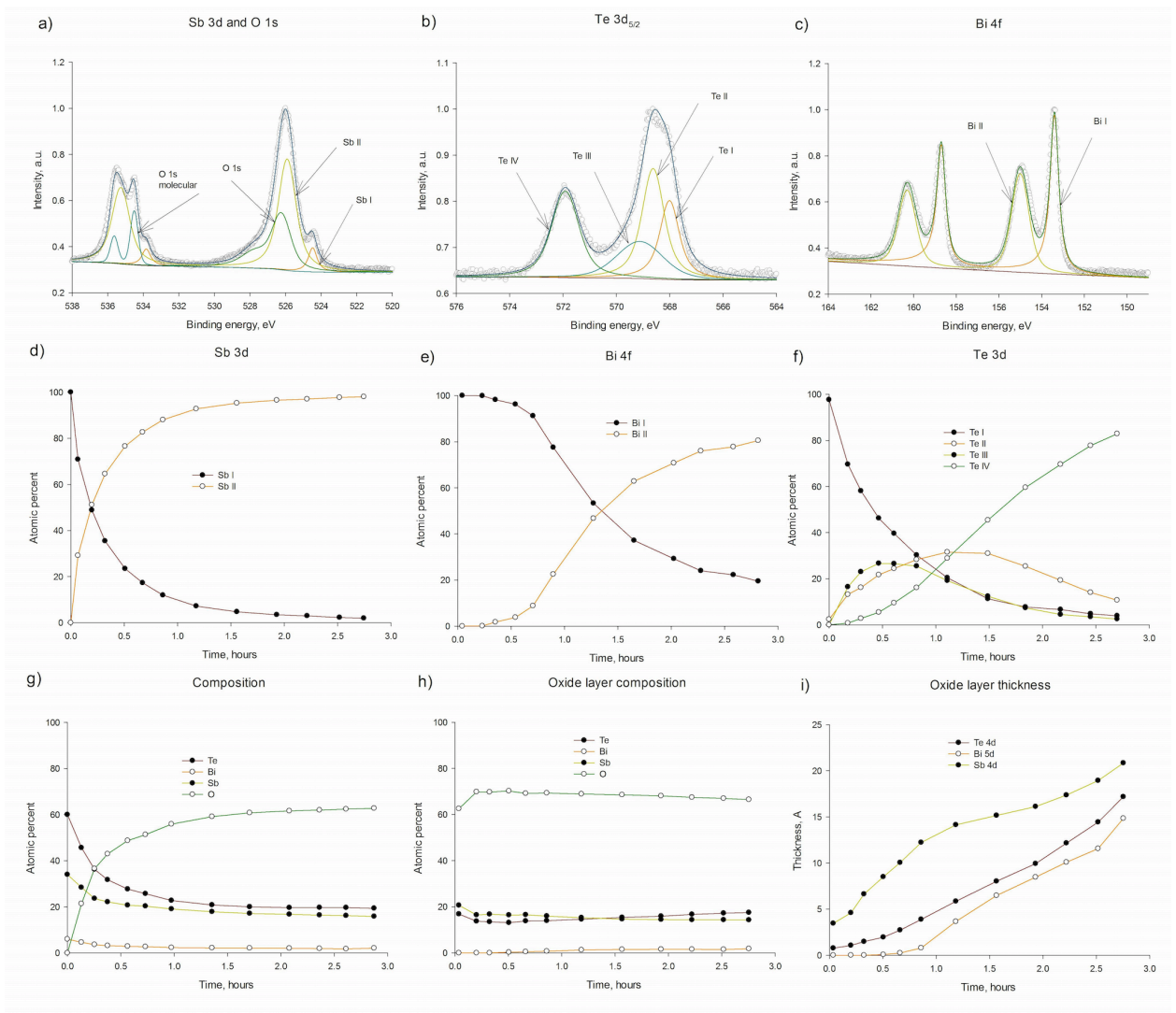Fig. S10. The oxidation kinetics measured in situ for the $(Bi_{0.45}Sb_{0.55})_2Te_3$ crystal surface (hv=750 eV).

9

Fig. S11. The oxidation kinetics measured in situ for the $(Bi_{0.15}Sb_{0.85})_2Te_3$ crystal surface (hv=750 eV).